

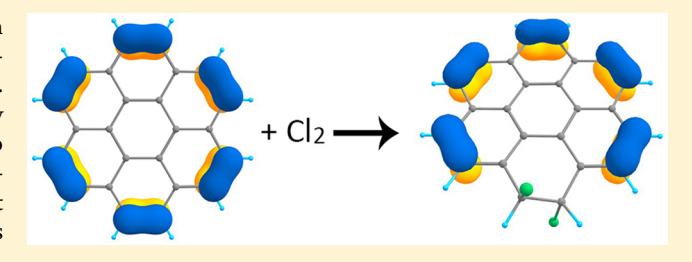
# Insight into The Nature of Rim Bonds in Coronene

Nikita Fedik and Alexander I. Boldyrev\*

Department of Chemistry and Biochemistry, Utah State University, Logan, Utah 84322, United States

Supporting Information

ABSTRACT: Coronene is known in chemistry as an aromatic or even superaromatic molecule while it has 24  $\pi$ electrons which does not conform to the 4n + 2 Huckel's rule. Chemical bonding description of it is not settled in chemistry and five models were reported in the literature. According to our model, coronene has two concentric  $\pi$ -systems responsible for aromaticity inside of the molecule. In addition to that there are six peripheral 2c-2e  $\pi$ -bonds, which makes coronene aliphatic/aromatic at the same time. However,



recent experiments and calculations put in question the presence of peripheral  $\pi$ -bonds. In order to resolve this issue, we computationally studied reaction mechanism of the Cl<sub>2</sub> molecule with C<sub>2</sub>H<sub>4</sub>, C<sub>6</sub>H<sub>6</sub>, and C<sub>24</sub>H<sub>12</sub>. As it turned out, coronene behaves in a way similar to ethylene by adding Cl<sub>2</sub> molecule. Thus, it proves that coronene indeed has peripheral double bonds which is also consistent with its experimental geometrical features. Our chemical bonding model allows to identify the most reactive atoms in coronene and other PAHs; therefore, it is a matter of importance for combustion and soot formation studies.

#### INTRODUCTION

Coronene  $C_{12}H_{24}$  is one of the most remarkable and intriguing molecules in organic chemistry. <sup>1–10</sup> Although it was first synthesized almost a century ago<sup>11</sup> it is still in focus<sup>4-6,12</sup> because of its unusual structure which remains a conundrum. As a big planar polycyclic molecule formally containing 24  $\pi$ electrons, coronene does not correspond to aromatic molecules which follow the 4n + 2 Huckel's rule so its wellknown experimental stability could not be theoretically substantiated by simple counting of conjugated system  $\pi$ electrons. Moreover, six rim bonds have noticeably shorter length, than other ones (Figure 1) and they are close to the double bond C=C in ethylene 1.3305 Å. This fact might indicate that these particular bonds have double bond character up to significant extent.

Today we have a few possible interpretations of coronene electronic structure (Figure 2).

One can infer from models 2, 3, and 5 that they do not reflect completely coronene geometrical features. Models 2 and 5 do not show six rim  $\pi$ -double bonds. Model 1 has some peripheral  $\pi$ -double bonding, but it is not as pronounced as in models 3 and 4. Model 3 does not describe correctly the  $\pi$ bonding inside of the coronene.

Last year there was a publication 16 on synthesis and characterization of persulfurated coronene C<sub>24</sub>S<sub>12</sub> also known as Sulflower instantly attracted attention due to its unusual high-symmetric and esthetic structure and prospective electrochemical properties. Moreover, it was named the molecule of the 2017 year. 17 Data regarding synthesis of Sulflower demonstrates that on the first steps it was fully chlorinated in the presence of Lewis acids giving structure  $C_{24}Cl_{12}$ ,  $D_{3d}$  by the electrophilic substitution which seems to be solid evidence

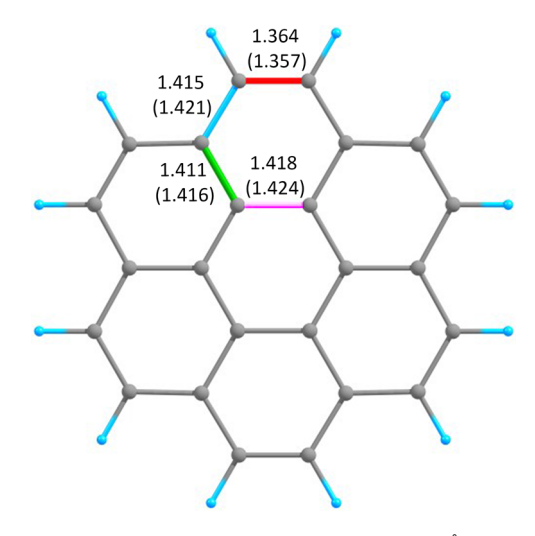


Figure 1. Bond lengths in coronene. All values are in Å. Upper values are obtained at the PBE0/cc-pVTZ level of theory, bottom ones (in parentheses) are experimental averages from X-ray data 14 assuming  $D_{6h}$  symmetry of coronene. C atoms are gray; H atoms are blue. Red bond (1.357) refers to peripheral or rim bond, blue one (1.421) to flank, and green one (1.416) to spoke, and pink one (1.424) refers to hub or central hexagon bond.

that it is a typical aromatic compound without any rim double bonds (Figure 3).

At first sight, Sulflower synthesis only made the coronene puzzle more tangled. On the one hand C24H12 was electro-

Received: August 15, 2018 Revised: October 5, 2018 Published: October 8, 2018

8585

The Journal of Physical Chemistry A

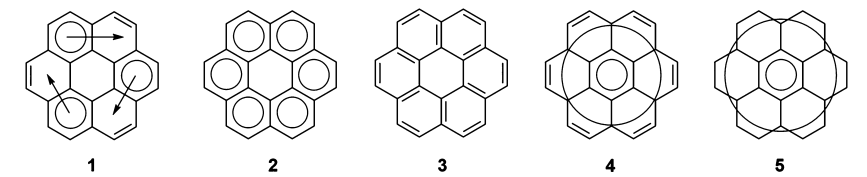


**Figure 2.** Different chemical bonding models of the coronene. Model **1** is a Kekule-like structure with arrows marking Clar sextet migration. Model **2** was suggested by Schleyer and co-workers. Model **3** was presented by England and Ruedenberg. Model **4** was obtained by Boldyrev and Zubarev using the AdNDP method. Model **5** was obtained by Zhai and co-workers using the AdNDP method. Model **5** was obtained by Zhai and co-workers using the AdNDP method.

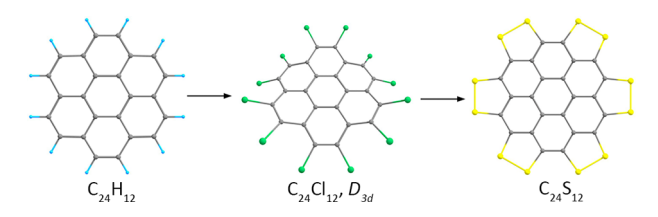


**Figure 3.** Simplified synthetic pathway of  $C_{24}S_{12}$ . Here and elsewhere C atoms are gray, H atoms are blue, Cl atoms are green, and S atoms are yellow.

philically substituted, which is a tendency of aromatic molecules. On the other hand, we have to keep in mind that presence of double peripheral bonds usually means an inclination to electrophilic addition reactions.

Because of lack of agreement between above-mentioned facts we feel necessity to resume the discussion which model of coronene chemical bonding is more pronounced (Figure 2). To answer to the question whether the coronene possess double bonds or not we suggest reactivity-based theoretical approach. We believe that this research will help us not only understand the nature of coronene structure more deeply, but also could be important for rationalizing the reactivity of other PAHs. Exploring reactive sites of PAHs plays crucial role in modern ecology, especially in branches regarding combustion and soot formation. <sup>18–23</sup>

In this article we decided to check the presence of the *rim* double bonds in coronene through the calculations of the reaction pathways of chlorination for coronene  $C_{24}H_{12}$ , ethylene  $C_2H_4$  and benzene  $C_6H_6$ . It is well-known that  $Cl_2$  molecule reacts with the  $C_2H_4$  producing the adduct  $C_2H_4Cl_2$  while  $Cl_2$  reacts with  $C_6H_6$  leading to monosubstituted benzene  $C_6H_5Cl$  and HCl. We hope that pathway of the reaction of  $Cl_2$  with  $C_{24}H_{12}$  will yield one of these mechanisms thus giving us the evidence of the presence or absence of the peripheral double bonds.

#### COMPUTATIONAL SECTION

All calculations were carried out at the PBE0/cc-pVTZ<sup>24–26</sup> level of theory using the software packages Gaussian 09. <sup>27</sup> All the structures were optimized up to default gradient value of  $10^{-7}$  hartree/bohr correspond to energy minima if the other is not specified. The nature of stationary points was evaluated by the calculations of analytical frequencies. The minimal energy pathways (MEPs) of reactions were obtained by the gradient descent from the transition states in the forward and backward directions of the imaginary frequencies vectors scaled by 0.1 coefficient. All the calculations were done in gas phase under 1 atm pressure and 298 K degrees. For the molecules  $C_{24}H_{12}$ ,  $D^{ch}$ ,  $C_{24}Cl_{12}$ ,  $D_{3d}$ ,  $C_{24}S_{12}$ ,  $D_{6h}$ ,  $C_{24}H_{12}Cl_{12}$ ,  $D_{3d}$  and  $C_{24}H_{12}Cl_{12}$ ,  $D_6$  wave function stability was checked. The search of transition states was based on Berny algorithm. <sup>28</sup> To perform chemical bonding analysis the AdNDP software was applied. <sup>3,4</sup>

Canonical MO and NBO $^{29-31}$  analysis for AdNDP were conducted at the PBE0/6-311G\*\*//PBE0/cc-pVTZ level of theory. Both general and directed methods of search for multicenter bonds were implemented according to the techniques described earlier in works.<sup>3,4</sup> Additionally NICS inidices<sup>32-35</sup> were calculated at PBE0/cc-pVTZ for the systems  $C_{24}H_{12}$ ,  $C_{24}H_{12}Cl_2$ , and  $C_{24}H_{12}Cl_{12}$ ,  $D_6$ .

## RESULTS

First we considered the chemical bonding picture in coronene  $C_{24}H_{12}$  and its derivatives synthesized in recent years. <sup>16</sup> Bonding pattern for coronene obtained within PBE0/6-311G\*\*/PBE0/cc-pVTZ methods has no qualitative or quantitative differences from the previously reported ones (Figure 4). <sup>3,4</sup> According to this analysis, in coronene we have

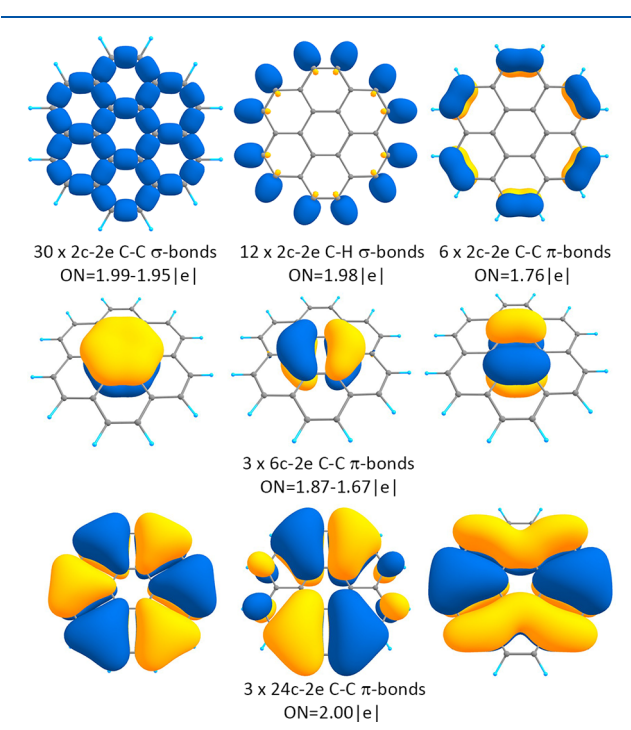


**Figure 4.** AdNDP analysis for  $C_{24}H_{12}$ . Thirty 2c-2e C-C σ-bonds, 12 2c-2e C-H σ-bonds, and six 2c-2e C-C  $\pi$ -bonds (upper line) superimposed on the molecular framework, three 6c-2e C-C  $\pi$ -bonds on the central hexagon (central line), and three 24c-2e C-C  $\pi$ -bonds delocalized on all C atoms (bottom line).

30 2c–2e C–C  $\sigma$ -bonds, 12 2c–2e C–H  $\sigma$ -bonds, six 2c–2e C–C  $\pi$ -bonds, and three 6c–2e C–C  $\pi$ -bonds on the hub hexagon and three 24c–2e C–C  $\pi$ -bonds delocalized on all C atoms. Since the occupation numbers (ON) for the 2c–2e  $\pi$ -bonds are somewhat low it signals that other C atoms may contribute to these bonds. Including the two sides carbon atoms causes increasing of occupation numbers up to 1.99 lel

in the 4c-2e  $\pi$ -bonds without any significant impact on shape or ON of other bonds (for full picture of the 4c-2e bonds see Supporting Information, Figure S1). The difference between 1.99 lel (4c-2e) and 1.76 lel (2c-2e) shows the effect of conjugation of the 2c-2e  $\pi$ -bond with the neighboring atoms.

In the structure  $C_{24}Cl_{12}$ ,  $D_{3d}$ , the AdNDP method recovered the chemical bonding pattern which is very close to  $C_{24}H_{12}$  even though  $C_{24}Cl_{12}$ ,  $D_{3d}$  is not planar at all (Figure 5).

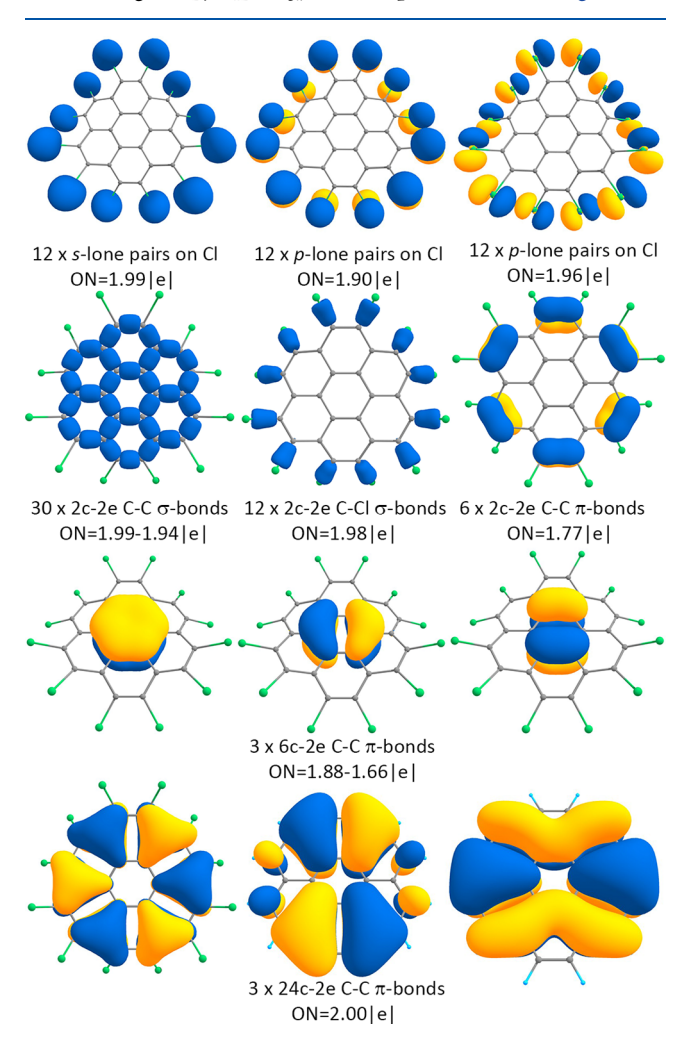


**Figure 5.** AdNDP analysis for  $C_{24}Cl_{12}$ ,  $D_{3d}$ . Twelve lone pairs of *s*-type and 24 of *p*-type located on 12 Cl atoms, (upper line), 30 2c–2e C–C  $\sigma$ -bonds, 12 2c–2e C–H  $\sigma$ -bonds, and six 2c–2e C–C  $\pi$ -bonds (second line) superimposed on the molecular framework, three 6c–2e C–C  $\pi$ -bonds on the central hexagon (third line), and three 24c–2e C–C  $\pi$ -bonds delocalized over all C atoms (bottom line).

According to our calculations, Cl atoms were located out of plane by 0.963 Å and C atoms by 0.349 Å. We also performed the AdNDP analysis for the  $C_{24}S_{12}$ , but since we got a very similar bonding picture to both  $C_{24}H_{12}$  and  $C_{24}Cl_{12}$ ,  $D_{3d}$ , we placed it in the Supporting Information (Figure S2).

## MEPS STUDY

At the next stage we studied minimal energy pathways (MEPs) and analyzed monochlorination of ethylene  $C_2H_4$ . It goes as a three-step mechanism initiating with addition ( $C_2H_4Cl_2$ -TS1) of a chorine radical to the double bond forming triangle complex  $C_2H_4Cl\cdot Cl$  (Figure 6, line a). Furthermore, intermediate  $C_2H_4Cl\cdot Cl$  adds second chlorine radical ( $C_2H_4\cdot Cl\cdot Cl$ )

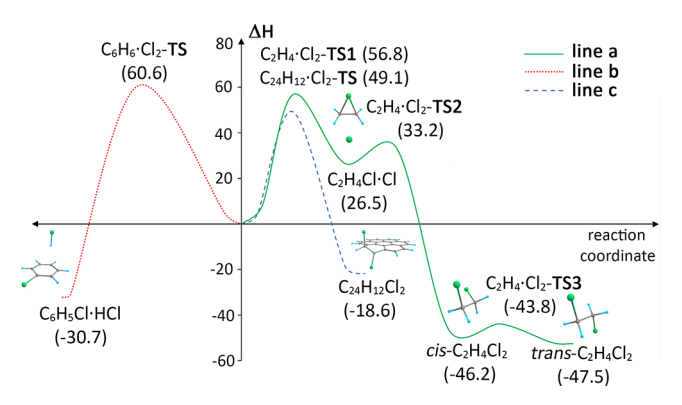


**Figure 6.** Calculated at PBE0/cc-pVTZ reactions pathways of monochlorination. Green solid line (line a) corresponds to  $C_2H_4$  MEP, red round dot (line b) to  $C_6H_6$  and blue dash (line c) to  $C_{24}H_{12}$ . Origin of coordinates and zero  $\Delta H$  value are on the intersection of axis. As the initial point of all MEPs sum of energies of separated reactants were taken.  $\Delta H$  is in kcal/mol and represents relative gas-phase enthalpy (values in parentheses). Transition states on the reaction coordinate are marked as **TSs**. Results of AdNDP analysis for structure  $C_{24}H_{12}Cl_2$  are depicted in Figure 7.

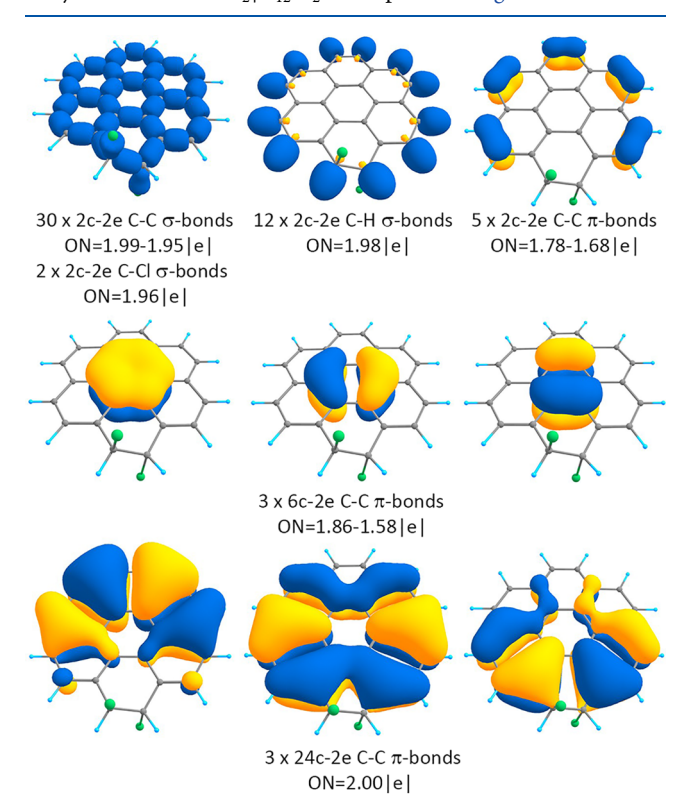


**Figure 7.** AdNDP analysis for  $C_{24}H_{12}Cl_2$ . Lone pairs of *s*-type and *p*-type on Cl atoms are omitted, 30 2c–2e C–C *σ*-bonds and two 2c–2e C–Cl *σ*-bonds, 12 2c–2e C–H *σ*-bonds and six 2c–2e C–C *π*-bonds (upper line) superimposed on the molecular framework, three 6c–2e C–C *π*-bonds on the central hexagon (third line), and three 24c–2e *π*-bonds delocalized over all carbon atoms (bottom line).

Cl<sub>2</sub>-TS2) which leads to the formation of *cis*-dichloroethylene *cis*-C<sub>2</sub>H<sub>4</sub>Cl<sub>2</sub>. After that sterically hindered cis-conformer *cis*-C<sub>2</sub>H<sub>4</sub>Cl<sub>2</sub> turns into the more stable *trans*-conformer *trans*-C<sub>2</sub>H<sub>4</sub> through the transition state C<sub>2</sub>H<sub>4</sub>Cl<sub>2</sub>-TS3. Then we studied chlorination of benzene C<sub>6</sub>H<sub>6</sub> (Figure 6, line b). The steepest descent alongside the imaginary frequency of located transition state C<sub>6</sub>H<sub>6</sub>Cl<sub>2</sub>-TS leads us to the  $\sigma$ -complex in which

during optimization procedure proton migrates from sp<sup>3</sup>-hybridized C atom to Cl radical forming  $\pi$ -postreaction complex  $C_6H_5Cl\cdot HCl$ . Only substitution reaction pathway for  $C_6H_6$  was obtained since every optimization of transition state gave us  $C_6H_6Cl_2$ -TS. In case of coronene  $C_{24}H_{12}$  one-step addition reaction pathway was found (Figure 6, line c). The approach of  $Cl_2$  molecule (in transition state  $C_{24}H_{12}Cl_2$ -TS) to substrate  $C_{24}H_{12}$  results in the consecutive antiaddition of Cl radicals to which initial  $Cl_2$  molecule dissociates. It leads to the formation of adduct  $C_{24}H_{12}Cl_2$ .

# **■ THERMOCHEMICAL DATA**

At the next step we performed calculations for the heat of substitution and addition reactions (Figure 8). The product of

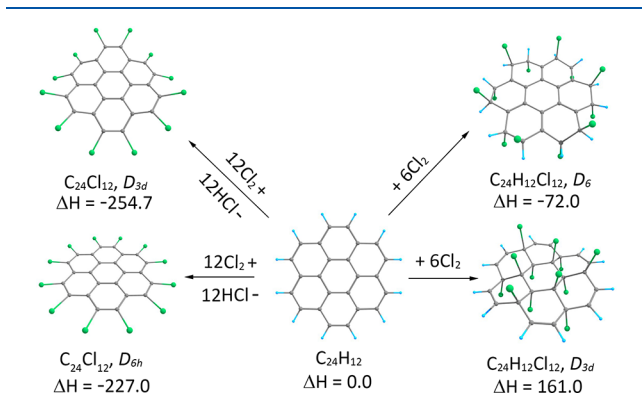


**Figure 8.** Thermodynamics data for coronene reactions of substitution (left side) or addition (right side).  $\Delta H$  is in kcal/mol and represents relative gas-phase enthalpy (values below structures). To calculate relative values electronic energies of the reactants above arrows were added to coronene and energies of below ones were added to products.

full substitution  $C_{24}Cl_{12}$ ,  $D_{3d}$ , is more stable than initial coronene  $C_{24}H_{12}$  by 254.7 kcal/mol while the hypothetical perfectly plane isomer  $C_{24}Cl_{12}$ ,  $D_{6h}$  is less stable by 27.7 kcal/mol thermodynamically than the nonplanar structure and has nine imaginary frequencies. As calculations showed, the structure  $C_{24}H_{12}Cl_{12}$ ,  $D_6$ , is exothermic meanwhile the speculative product  $C_{24}H_{12}Cl_{12}$ ,  $D_{3d}$  of the addition to the *spoke* bonds is energetically absolutely not feasible.

Chemical bonding pattern revealed by AdNDP of the molecule  $C_{24}H_{12}Cl_{12}$ ,  $D_6$  is represented in Figure 9.

# NICS CALCULATIONS

To assess aromaticity in initial coronene  $C_{24}H_{12}$  and its products of addition ( $C_{24}H_{12}Cl_2$  and  $C_{24}H_{12}Cl_{12}$ ,  $D_6$ ) NICS<sub>zz</sub> indices were calculated at the PBE0/cc-pVTZ level of theory (Supporting Information, Figure S3 and Tables S21–S23). For each system six NICS values were obtained from NICS(0.0)<sub>zz</sub> to NICS(1.0)<sub>zz</sub> using 0.2 Å increment.

# DISCUSSION

On the basis of the mechanism of chlorination for  $C_{24}H_{12}$ ,  $C_2H_4$ , and  $C_6H_6$  (Figure 6), we can discuss coronene electronic structure. Let us begin with the kinetic study of  $C_2H_4$  chlorination. We found the classical textbook mechanism which correlates well to previous theoretical investigation of ethylene halogenation MEP.<sup>36</sup> On the contrary,  $C_6H_6$  showed no inclination to addition reactions. As it was expected, it

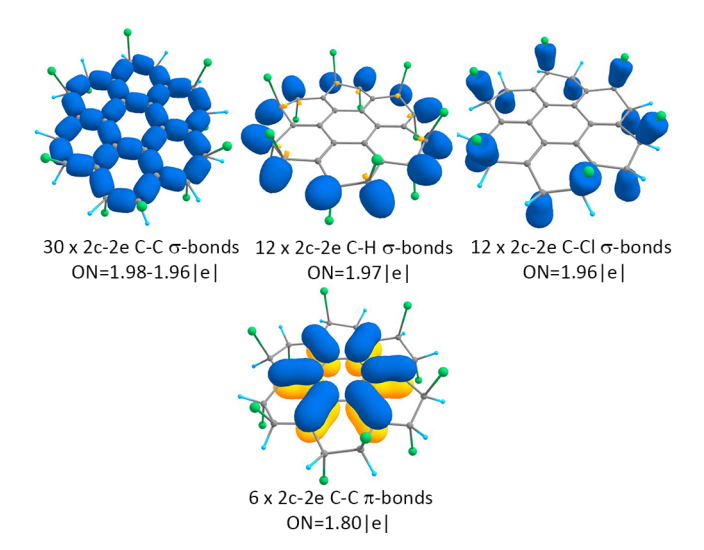


**Figure 9.** AdNDP analysis for  $C_{24}H_{12}Cl_{12}$ ,  $D_6$ . Lone pairs of s-type and p-type on Cl atoms are omitted, 30 2c-2e C-C σ-bonds, 12 2c-2e C-H σ-bonds and 12 2c-2e C-Cl σ-bonds (upper line) superimposed on the molecular framework, and six 2c-2e C-C  $\pi$ -bonds on the central hexagon (bottom line).

undergoes one-step substitution reaction very typical to organic aromatic compounds while transition state leading to addition reaction was not located at all. Now the question is, to which of them, ethylene or benzene, coronene is closer in its reactivity? According to calculations, coronene follows ethylene-like reaction path but undergoes it at one-step and with lower activation energy (Figure 6). Interestingly,  $C_{24}H_{12}$  does not form triangle complex as a first intermediate of electrophilic addition. Probably such facilitation of addition reaction caused by distortion of the high symmetrical carbon framework after the attachment of first chlorine radical (Figure 7). All the facts indicate that  $C_{24}H_{12}$  indeed behaves in the similar manner as ethylene and may form adducts in electrophilic reactions.

On the other hand, calculated thermochemical data reveals that reaction of the full substitution of coronene is more favorable than addition reaction of six Cl2 molecules (Figure 8). According to the AdNDP analysis, addition of even one Cl<sub>2</sub> molecule causes the noticeable deterioration of aromatic system in structure  $C_{24}H_{12}Cl_2$  (Figure 7). As we can see from chemical bonding picture, Cl2 addition not only consumes one of the  $\pi$ -bonds (just like in the case of ethylene) but also breaks symmetry of 24c-2e bonds appreciably depleting one of these bonds. It could be expected because 2c-2e  $\pi$ -bonds are not entirely isolated; in case of coronene they overlap with three aromatic 24c-2e bonds delocalized over all carbon atoms. This, indeed makes coronene one of the most exciting nonclassic structures. Being on the edge of two contrast properties it possesses both of them up to a certain extent. It should be noticed that monosubstituted coronene was synthesized many years ago in presences of Lewis acid.<sup>37</sup> Seemingly product of coronene chlorination heavily relies on reaction conditions thus giving us reason to hope that adduct C<sub>24</sub>H<sub>12</sub>Cl<sub>2</sub> could be experimentally

Obviously consequent addition of  $Cl_2$  to  $C_{24}H_{12}Cl_2$  will gradually drain concentric aromaticity causing further instability and the product  $C_{24}H_{12}Cl_{12}$ ,  $D_6$ , is an example. Complete addition does not have any crucial impacts on  $\sigma$ -framework

besides steric distortion whereas  $rim \pi$ -bonds are fully depleted as well as concentric aromaticity (Figure 9). These AdNDP results showing gradual depletion of aromaticity from initial coronene to product of complete addition are also in good agreement with NICS indices known as widely used aromaticity markers (Supporting Information, Figure S3, Tables S21–S23). 32–35

Residual density in structure  $C_{24}H_{12}Cl_{12}$ ,  $D_6$  was located in shape of six spoke  $\pi$ -bonds. It does not mean that  $C_{24}H_{12}Cl_{12}$  $D_{6i}$  is still very reactive since any further addition likely has to be highly endothermic due to steric reasons and extremely strong repulsion between chlorine atoms as in product  $C_{24}H_{12}Cl_{12}$ ,  $D_{3d}$  (Figure 8). Structure  $C_{24}H_{12}Cl_{12}$ ,  $D_{3d}$ correlates to the adduct of six Cl2 molecules to the C24H12 described by model 3 of England and Ruedenberg. Such addition is possible only in the case of full destruction of both aromatic circles since it consumes all the delocalized electrons to produce new twelve C–Cl  $\sigma$ -bonds. This result is consistent with the previous investigation, 12 where the authors considered hydrogenation of coronene. According to both experimental and theoretical methods, it was found that hydrogenation of the carbon atom involved in 2c-2e rim  $\pi$ -bonds is more kinetically and thermodynamically favorable than the hydrogenation of spoke bond carbon atoms. The lower preference of attack involving spoke and hub carbon atoms may be explained by the overlapping of the two concentric aromatic systems. In contrast to adducts  $C_{24}H_{12}Cl_{12}$ ,  $D_6$ , and  $C_{24}H_{12}Cl_{12}$ ,  $D_{3d}$ , fully substituted C24Cl12, D6 remains being aromatic as well as  $C_{24}S_{12}$  (Supporting Information, Figure S2).

As it was emphasized in the Introduction, recent model 5 does not recover six rim  $\pi$ -bonds and presents peripheral aromatic system consisting of 18 electrons. Formally it meets Huckel's rule but ignores crucial geometrical features and therefore chemical properties. For instance, predicted by MEPs calculations tendency to addition reactions.

## CONCLUSIONS

We believe that considered model reaction of C24H12 chlorination is a persuasive evidence of the existence of six  $C_{24}H_{12}$  peripheral  $\pi$ -bonds. Noticeably, model 1 also explains why the addition reaction is exothermic in coronene. According to this model the addition does not break the aromaticity of the system since the final product keeps the three Clar  $\pi$ -sextets.

If we return to Figure 2, now we see that models 2, 3, and 5 do not fully agree with the geometrical features of coronene. Apparently, the main purpose of good chemical bonding model is to serve as bridge between the nonintuitive laws of quantum mechanics and visual language understandable by chemists. Taking into account that our model represents both geometrical features and simple chemical properties we assume it as the most suitable for  $C_{24}H_{12}$ . We would like to believe that this study will be a breakthrough in coronene's puzzle solution. Also, we reckon that obtained results will help to detect most reactive sites of PAHs which are of the essential interests for the proper models of combustion and soot formation.  $^{18-23}\,\mathrm{We}$ plan to study chemical bonding in larger PAHs with the aim of developing a general simple representation of these kind of

We consider this case as the first example of application of AdNDP method to reactivity predictions. Although AdNDP at this moment does not operate with quantitative markers as for instance Fukui functions or reactivity indices, it is still a

powerful tool for making illustrative pictures of chemical bonding for wide audience of scientists.

#### ASSOCIATED CONTENT

# S Supporting Information

The Supporting Information is available free of charge on the ACS Publications website at DOI: 10.1021/acs.jpca.8b07937.

AdNDP analysis for C<sub>24</sub>H<sub>12</sub> (4c-2e peripheral bonds recovered instead of 2c-2e) and  $C_{24}S_{12}$ , Cartesian coordinates for all structures mentioned and values of NICS for  $C_{24}H_{12}$ ,  $C_{24}H_{12}Cl_2$ , and  $C_{24}H_{12}Cl_{12}$ ,  $D_6$  (PDF)

## AUTHOR INFORMATION

#### **Corresponding Author**

\*(A.I.B.) E-mail: a.i.boldyrev@usu.edu.

ORCID ®

Alexander I. Boldyrev: 0000-0002-8277-3669

The authors declare no competing financial interest.

#### ACKNOWLEDGMENTS

This work was supported by the National Science Foundation (CHE-1664379).

#### REFERENCES

- (1) Fawcett, J. K.; Trotter, J. The Crystal and Molecular Structure of Coronene. Proc. R. Soc. London, Ser. A 1966, 289 (1418), 366-376.
- (2) Randić, M. Graph Theoretical Approach to  $\pi$ -Electron Currents in Polycyclic Conjugated Hydrocarbons. Chem. Phys. Lett. 2010, 500 (1-3), 123-127.
- (3) Zubarev, D. Y.; Boldyrev, A. I. Revealing Intuitively Assessable Chemical Bonding Patterns in Organic Aromatic Molecules via Adaptive Natural Density Partitioning. J. Org. Chem. 2008, 73 (23), 9251-9258.
- (4) Popov, I. A.; Boldyrev, A. I. Chemical Bonding in Coronene, Isocoronene, and Circumcoronene. Eur. J. Org. Chem. 2012, 2012, 3485 - 3491.
- (5) Kumar, A.; Duran, M.; Solà, M. Is Coronene Better Described by Clar's Aromatic  $\pi$ -Sextet Model or by the AdNDP Representation? *J.* Comput. Chem. 2017, 38 (18), 1606-1611.
- (6) Li, R.; You, X. R.; Wang, K.; Zhai, H. J. Nature of Bonding in Bowl-Like B36 Cluster Revisited: Concentric  $(6\pi+18\pi)$  Double Aromaticity and Reason for the Preference of a Hexagonal Hole in a Central Location. Chem. - Asian J. 2018, 13 (9), 1148-1156.
- (7) England, W.; Ruedenberg, K. Localized  $\pi$ -Orbitals, Pauling Bond Orders, and the Origin of Aromatic Stability. Theor. Chim. Acta 1971, 22 (2), 196-213.
- (8) Moran, D.; Stahl, F.; Bettinger, H. F.; Schaefer, H. F.; Schleyer, P. R. Towards Graphite: Magnetic Properties of Large Polybenzoid Hydrocarbons. J. Am. Chem. Soc. 2003, 125, 6746-6752.
- (9) Randić, M. Aromaticity of Polycyclic Conjugated Hydrocarbons. Chem. Rev. 2003, 103 (9), 3449-3605.
- (10) Berionni, G.; Wu, J. I. C.; Schleyer, P. V. R. Aromaticity Evaluations of Planar [6] Radialenes. Org. Lett. 2014, 16 (23), 6116-
- (11) Newman, M. S. A. New Synthesis of Coronene. J. Am. Chem. Soc. 1940, 62 (7), 1683–1687.
- (12) Cazaux, S.; Boschman, L.; Rougeau, N.; Reitsma, G.; Hoekstra, R.; Teillet-Billy, D.; Morisset, S.; Spaans, M.; Schlathölter, T. The Sequence to Hydrogenate Coronene Cations: A Journey Guided by Magic Numbers. Sci. Rep. 2016, 6, 1-7.
- (13) Craig, N. C.; Groner, P.; McKean, D. C. Equilibrium Structures for Butadiene and Ethylene: Compelling Evidence for II-Electron Delocalization in Butadiene. J. Phys. Chem. A 2006, 110 (23), 7461-7469.

- (14) Krygowski, T. M.; Cyrański, M.; Ciesielski, A.; Świrska, B.; Leszczyński, P. Separation of the Energetic and Geometric Contributions to Aromaticity. 2. Analysis of the Aromatic Character of Benzene Rings in Their Various Topological Environments in the Benzenoid Hydrocarbons. Crystal and Molecular Structure of Coronene. *J. Chem. Inf. Comput. Sci.* 1996, 36 (6), 1135–1141.
- (15) Clar, E.; Sanigök, Ü.; Zander, M. NMR Studies of Perylene and Coronene Derivatives. *Tetrahedron* **1968**, 24 (7), 2817–2823.
- (16) Dong, R.; Pfeffermann, M.; Skidin, D.; Wang, F.; Fu, Y.; Narita, A.; Tommasini, M.; Moresco, F.; Cuniberti, G.; Berger, R.; et al. Persulfurated Coronene: A New Generation of "Sulflower". *J. Am. Chem. Soc.* **2017**, *139* (6), 2168–2171.
- (17) Ritter, S. K. Molecules of the Year. C&EN highlights some of the coolest compounds reported in 2017. https://cen.acs.org/articles/95/i49/molecules-of-the-year-2017.html (accessed 08.03.2018).
- (18) Frenklach, M. Reaction Mechanism of Soot Formation in Flames. *Phys. Chem. Chem. Phys.* **2002**, *4* (11), 2028–2037.
- (19) Schuetz, C. A.; Frenklach, M. Nucleation of Soot: Molecular Dynamics Simulations of Pyrene Dimerization. *Proc. Combust. Inst.* **2002**, 29 (2), 2307–2314.
- (20) Whitesides, R.; Frenklach, M. Detailed Kinetic Monte Carlo Simulations of Graphene-Edge Growth. *J. Phys. Chem. A* **2010**, *114* (2), 689–703.
- (21) Frenklach, M.; Liu, Z.; Singh, R. I.; Galimova, G. R.; Azyazov, V. N.; Mebel, A. M. Detailed, Sterically-Resolved Modeling of Soot Oxidation: Role of O Atoms, Interplay with Particle Nanostructure, and Emergence of Inner Particle Burning. *Combust. Flame* **2018**, *188*, 284–306.
- (22) Thomas, A. M.; Lucas, M.; Yang, T.; Kaiser, R. I.; Fuentes, L.; Belisario-Lara, D.; Mebel, A. M. A Free-Radical Pathway to Hydrogenated Phenanthrene in Molecular Clouds—Low Temperature Growth of Polycyclic Aromatic Hydrocarbons. *ChemPhysChem* **2017**, *18* (15), 1971–1976.
- (23) Lucas, M.; Thomas, A. M.; Kaiser, R. I.; Bashkirov, E. K.; Azyazov, V. N.; Mebel, A. M. Combined Experimental and Computational Investigation of the Elementary Reaction of Ground State Atomic Carbon (C;<sup>3</sup>P<sub>j</sub>) with Pyridine (C<sub>5</sub>H<sub>5</sub>N; X<sup>1</sup>A<sub>1</sub>) via Ring Expansion and Ring Degradation Pa. *J. Phys. Chem. A* **2018**, *122* (12), 3128–3139.
- (24) Adamo, C.; Barone, V. Toward Reliable Density Functional Methods without Adjustable Parameters: The PBE0Model. *J. Chem. Phys.* **1999**, *110* (13), 6158–6170.
- (25) Dunning, T. H. Gaussian Basis Sets for Use in Correlated Molecular Calculations. I. The Atoms Boron through Neon and Hydrogen. *J. Chem. Phys.* **1989**, *90* (2), 1007–1023.
- (26) Woon, D. E.; Dunning, T. H. Gaussian Basis Sets for Use in Correlated Molecular Calculations. III. The Atoms Aluminum through Argon. *J. Chem. Phys.* **1993**, *98* (2), 1358–1371.
- (27) Frisch, M. J.; et al. Gaussian 09; Gaussian, Inc.: Wallingford, CT, 2013.
- (28) Schlegel, H. B. Optimization of Equalibrium Geometries and Transition Structures. *Adv. Chem. Phys.* **2007**, *67* (2), 249.
- (29) Glendening, E. D., Reed, A. E., Carpenter, J. E., Weinhold, F. NBO, Version 3.1; .
- (30) Foster, J. P.; Weinhold, F. J. Am. Chem. Soc. 1980, 102 (24), 7211–7218.
- (31) Reed, A. E.; Curtiss, L. A.; Weinhold, F. Intermolecular Interactions from a Natural Bond Orbital, Donor-Acceptor Viewpoint. *Chem. Rev.* **1988**, *88* (6), 899–926.
- (32) Chen, Z.; Wannere, C. S.; Puchta, R.; Schleyer, P. v. R.; et al. Nucleus-Independent Chemical Shifts (NICS) as an Aromaticity Criterion. *Chem. Rev.* **2005**, *105*, 3842–3888.
- (33) Stanger, A. Nucleus-Independent Chemical Shifts (NICS): Distance Dependence and Revised Criteria for Aromaticity and Antiaromaticity. *J. Org. Chem.* **2006**, *71*, 883–893.
- (34) Berionni, G.; Wu, J. I. C.; Schleyer, P. V. R. Aromaticity Evaluations of Planar [6] Radialenes. *Org. Lett.* **2014**, *16* (23), 6116–6119.

- (35) Solà, M.; Feixas, F.; Jiménez-halla, J. O. C.; Matito, E.; Poater, J. A Critical Assessment of the Performance of Magnetic and Electronic Indices of Aromaticity. *Symmetry* **2010**, *2*, 1156–1179.
- (36) Islam, S. M.; Poirier, R. Á. New Insights into the Bromination Reaction for a Series of Alkenes a Computational Study. *J. Phys. Chem. A* **2007**, *111* (50), 13218–13232.
- (37) Nilsson, U. L.; Colmsjö, A. L. Retention Characteristics of Chlorinated Polycyclic Aromatic Hydrocarbons in Normal Phase HPLC. I. Chloro-Added PAHs. *Chromatographia* **1991**, 32 (7–8), 334–340.